Acousto-optics studied in polaritonic photonic crystals

Mahi R. Singh and C. Racknor
Department of Physics and Astronomy, The University of Western Ontario, London, Ontario, Canada N6A 3K7
(Received 28 July 2010; revised manuscript received 20 September 2010; published 21 October 2010)

We have studied the acousto-optic effect on the photon transmission and the spontaneous emission in polaritonic photonic crystal. We have considered that photonic crystals are fabricated from polaritonic materials such as GaP, MgO, $LiNbO_3$, and $LiTaO_3$. A two-level quantum dot is doped in a polaritonic crystal to study the decay rate of the spontaneous emission. The decay rate of quantum dots, band structure, and photon transmission coefficient have been calculated. It is found that band-gap width and the decay rate of quantum dots depends strongly on the high-frequency dielectric constant of the polaritonic crystals while the photonic band edges vary inversely by the ratio of longitudinal- to transverse-optical phonon energies. The spontaneous decay rate of the quantum dot can be controlled by the external strain field. This finding is significant because it is well known that the spontaneous emission is source of undesirable noise in different types of electronic and optical devices. Finally, we have also found the system can be switched from transmitting state to reflecting state by applying an external strain field. These are distinct and interesting results and can be used to fabricate new types of photonic couplers and fibers which in turn can be used to fabricate all photonic switches.

DOI: 10.1103/PhysRevB.82.155130 PACS number(s): 42.70.Qs, 42.55.Tv, 78.20.Bh

I. INTRODUCTION

In this paper we investigate the acousto-optic effect in photonic crystals fabricated from polaritonic materials. Interest in polaritonic materials lies in their potential to create new devices with operational frequencies ranging from hundreds of gigahertz to several terahertz (THz), which is the regime connecting photonics and electronics. Devices made from polaritonic materials would not suffer from the technological and physical barriers that limit speed in electronic devices, nor would they require lossy integration of light sources and guiding structures as in photonic systems.[1,2] Polaritonic materials can be semiconductors, oxide crystals, glasses, organic, and inorganic materials.[3] Applications for these materials will have a wide range, including high-bandwidth signal processing, THz imaging, and THz spectroscopy.[1,2]

Polaritons are quasiparticles formed by strong coupling of an incident transverse electromagnetic wave with transverse-optical phonons in the host material. Interest in studying polaritons has increased as of late. Maragkou *et al.*[4] have proposed that polaritonic materials may be used to create lasers that operate at reduced thresholds. Polariton band gaps in the THz range have been studied in periodic and quasiperiodic multilayer systems.[5] Reflection and absorption measurements have also been obtained for polaritonic materials in the THz-frequency range.[6] Polaritonic waveguides and resonators have been fabricated from $LiNbO_3$ and $LiTaO_3$ host crystals[1,2,7] while polaritonic wires made from an isotropic dielectric material coated with metal have also been investigated.[8] In our own recent work, we have shown that suppression of spontaneous emission occurs when a quantum dot is placed within a polaritonic material,[9,10] and we have studied the optoelectronic behavior of a polaritonic nanowire in the context of developing all-optical switches.[11]

In dielectric photonic crystals, high dielectric contrast is required for a full photonic band gap to form. For example, inverse opal photonic crystals require dielectric contrast of a factor of 8 to obtain a photonic band gap in the optical regime. This restriction causes a great deal of difficulty in terms of fabrication. Materials with energy-dependent dielectric constants, such as polaritonic materials, are the best alternative to overcome this barrier. Here we are considering photonic crystals fabricated using polaritonic materials. Photonic crystals are periodic nanostructures that possess photonic band gaps, which prohibit light propagation within a certain range of frequencies. In a photonic crystal, photonic band gaps are formed due to a periodic variation in refractive index, whereas in polaritonic materials the energy gap is due to coupling between the optical transverse phonons and photons. The effective index of refraction of a polaritonic material is therefore dependent on the frequency of an incident photon.

Recently, some work has been done on polaritonic photonic crystals.[12–24] For example, Huang *et al.*[12–14] have demonstrated that polaritonic photonic crystals will exhibit near-dispersionless bandwidth field localization in the polaritonic material and metal-like bands with complete flux expulsion in an extremely small frequency interval around the characteristic phonon frequency. Sigalas *et al.*[15] have calculated the transmission coefficient for a two-dimensional (2D) square lattice of GaAs and air and found it to have a band gap to be in the THz range. Zeng *et al.*[17] have used 2D polaritonic photonic crystals as waveguides and showed that propagation loss decays with increasing waveguide wall thickness. Högström and Ribbing[18] have verified the presence of a polaritonic band gap for thicknesses of one-dimensional photonic crystals lower than the wavelength for SiO_2/Si and SiO_2/air.

Furthermore, Kuzmiak *et al.*[19] calculated the photonic band structure for an infinite array of GaAs rods in a vacuum. They found that for larger values of the volume filling fraction, the dispersion relation produced a complete 2D photonic band gap for transverse electric electromagnetic waves, but not transverse magnetic waves. Rung and Ribbing[20] showed that in a polaritonic photonic crystal, the photonic gap can be shifted across the polaritonic gap by

varying the crystal's lattice constant. Rung *et al.*[21] have also calculated the band structure for a 2D photonic crystal of ceramic beryllium oxide, demonstrating the appearance and disappearance of complete photonic band gaps upon changing the packing fraction and the lattice constant. Chern *et al.*[22] used an interfacial operator approach to study the effect of structural and polaritonic parameters on four different polaritonic photonic crystal structures. Gantzounis and Stefanou[23] used layer-multiple scattering to study the optical properties of three-dimensional (3D) polaritonic photonic crystals and their transmission characteristics. In addition, they[24] also studied and the optical response of finite slabs of 2D and 3D periodic structures of air cavities in polaritonic materials, which revealed existence of strong resonant modes. The on-shell layer-multiple-scattering method is ideally suited to polaritonic photonic crystals for calculating complex frequency band structure, transmittance, reflectance, and absorbance of finite slabs of crystal. This method could be used to describe actual transmission experiments.

In this paper we have also studied the acousto-optic effect on the photon transmission and the spontaneous emission of quantum dots doped in a polaritonic photonic crystal. Recently there has been considerable interest in studying the acousto-optic effect in photonic crystals.[25–28] For example, Courjal *et al.*[25] have studied an active 2D lithium niobate photonic crystal driven by stationary Rayleigh surface acoustic waves. The configuration relies on two interdigital transducers that modulate the refractive index through the acousto-optic effect. Their experiments showed an enhancement of the elasto-optical interaction by a factor of 61.

The acousto-optic effect has recently been investigated in photonic crystal fibers.[26,27] For example, Haakestad and Engan[26] have studied experimentally the acoustic and acousto-optic properties of a weakly multimode solid core photonic crystal fiber. The phase velocity of the lowest order flexural acoustic mode is measured as a function of frequency. Acousto-optic interaction is used to couple light from the lowest order to the first higher order optical modes of the solid core fiber. Dainese *et al.*[27] have explored stimulated Brillouin scattering in glass photonic crystal fibers with subwavelength-scale solid silica glass cores. They found that Brillouin scattering is strongly affected by acousto-optical effect. Lim *et al.*[28] have measured the multiple resonance peaks in an all-fiber acousto-optic tunable filter built with a photonic crystal fiber. They explained their experiments by using physics of the acousto-optic mode coupling.

To study the suppression of spontaneous emission we have doped a two-level quantum dot in a polaritonic photonic crystal. The decay rate of the quantum dot due to spontaneous emission has been calculated using the Schrödinger equation method. The band structure of the polaritonic photonic crystals are calculated using the model proposed by John and Wang.[29] This model has been widely used to study the optical properties of photonic crystals[9,30–39] and correctly predicts the behavior of their band structure for these materials.

Numerical calculations are performed for polaritonic photonic crystals fabricated from GaP, MgO, $LiNbO_3$, and $LiTaO_3$. It is found that the photonic band-gap width and the decay rate of quantum dots depends strongly on the high-frequency dielectric constant, ϵ_∞, of the polaritonic material, while the photonic band edges vary inversely with the factor $\epsilon_\infty \varepsilon_L^2/\varepsilon_T^2$, where ε_L and ε_T are the longitudinal- and transverse-optical phonon energies of the host material, respectively. The decay rate and transmission coefficient have been calculated in the presence of an external strain field. It is found that the decay rate increases when the resonance energy of the quantum dot lies within the lower photon propagation band. On the other hand, when the resonance energy lies in the upper band the decay rate decreases. In other words the spontaneous emission of the quantum dot can be controlled by the external strain field. This finding is significant because spontaneous emission is the source of undesirable noise in different types of electronic and optical devices. The control of the spontaneous emission also plays a very significant role in quantum computation and quantum information processing.

We have also found the polaritonic photonic crystals can be switched from a transmitting state to a reflecting state by applying an external strain field. The findings presented in this paper can be used to fabricate different types of optical switches. When the system is in reflecting state it can be considered in the OFF position, and when the system is in transmitting state it can be considered as ON. The present research opens opportunities for controlling light-sound interactions in photonic crystals and optical fibers made from photonic crystals.

II. POLARITONIC PHOTONIC CRYSTALS

We consider that a photonic crystal is made from dielectric spheres which are arranged periodically in a background polaritonic material, where the polaritonic background material has a frequency-dependent refractive index. For simplicity, the dielectric material is taken as air. This type of crystal is similar in form to Yablonovite, which was fabricated by drilling air spheres into silica in a periodic manner.[40] Here the radius of the dielectric spheres is taken as r_s and the lattice constant of the crystal is denoted by L.

The index of refraction of a polaritonic material is frequency dependent and is written as[14]

$$n_p(\varepsilon_k) = \left[\epsilon_\infty \frac{(\varepsilon_k^2 - \varepsilon_L^2 - i\gamma\varepsilon_k)}{(\varepsilon_k^2 - \varepsilon_T^2 - i\gamma\varepsilon_k)} \right]^{1/2}, \tag{1}$$

where ε_T and ε_L are is the transverse and longitudinal phonon energy, respectively. Constant ϵ_∞ is the high-frequency dielectric constant which is the contribution due to ion core electrons and γ is the energy loss factor. The band structure of the polaritonic photonic crystal considered here has been modeled using the technique developed by John and Wang.[29] This model has been used widely to study the quantum optics of photonic crystals.[9,30–39] According to this model the band structure of the photonic crystal is given as

$$\cos(kL) = F(\varepsilon_k), \tag{2}$$

where

$$F(\varepsilon_k) = \sum_{\pm} \left[\pm \left\{ \frac{[n_p(\varepsilon_k) \pm n_s]^2}{4n_p(\varepsilon_k)n_s} \right\} \times \cos\left\{ \frac{\varepsilon_k[n_p(\varepsilon_k)2a \pm n_s(L-2a)]}{\hbar c} \right\} \right]. \quad (3)$$

Here ε_k is energy and k the Bloch wave vector of photons in the photonic crystal. The physical parameter a is chosen where $r_s = \frac{1}{2}a$ and r_s is the radius of the spheres. n_p is the refractive index of the polaritonic background material and n_s is that of the spheres.

III. ACOUSTO-OPTIC EFFECT

When an external mechanical strain (i.e., acoustic wave) is applied to a polaritonic material, its refractive index is modified due to photon-phonon interaction. This is known as the acousto-optic effect. Let us apply an acoustic (phonon) wave to our system with intensity I_a. The intensity of the acoustic wave is written as

$$I_a = \frac{1}{2}\rho v_s^3 S_a^2, \quad (4)$$

where ρ is the density, v_s is the phonon wave speed, and S_a is the magnitude of the strain.

Let us consider that a longitudinal acoustic wave is traveling along the x direction and the displacement (deformation) of the material is u_x. The strain S_a is then defined as

$$S_a = \pm \frac{du_x}{dx}, \quad (5)$$

where + and − stand for the compression and dilation of the system, respectively. As the elastic material is deformed due to the external strain (acoustic wave), the optical impermeability η of the system is related to the strain as[41]

$$\Delta\eta = pS_a, \quad (6)$$

where p is called the photoelastic or acousto-optic constant. The optical impermeability is related to the dielectric constant ϵ of a material as

$$\eta = \sqrt{\frac{\epsilon_0}{\epsilon}}, \quad (7)$$

where ϵ_0 is the dielectric constant in a vacuum.

In the presence of the external strain the dielectric constant of the material is modified. Therefore, the refractive index of the system can be obtained by solving Maxwell's equations by using the coupled wave theory. The refractive index of the system is obtained as

$$n_T(\varepsilon_k) = n_p \left[\frac{\varepsilon_k^2 - \varepsilon_T^2 - i\gamma\varepsilon_k \pm \frac{1}{2}pS_a(\varepsilon_k^2 - \varepsilon_L^2 - i\gamma\varepsilon_k)}{\varepsilon_k^2 - \varepsilon_T^2 - i\gamma\varepsilon_k} \right]. \quad (8)$$

Note that if we neglect the effect of the external strain (i.e., $S_a = 0$) the above expression reduces to Eq. (8). Let us express S_a in terms of the intensity of strain field (acoustic wave) by rearranging Eq. (4), which gives

$$S_a = \left(\frac{2I_a}{\rho v_s^3} \right)^{1/2}. \quad (9)$$

Putting the above expression of S_a into Eq. (8) we find

$$n_T(\varepsilon_k) = n_p \left[\frac{\sqrt{\epsilon_\infty}(\varepsilon_k^2 - \varepsilon_T^2 - i\gamma\varepsilon_k) \pm \left(\frac{1}{2}\eta I_a\right)^{1/2}(\varepsilon_k^2 - \varepsilon_L^2 - i\gamma\varepsilon_k)}{\sqrt{\epsilon_\infty}(\varepsilon_k^2 - \varepsilon_T^2 - i\gamma\varepsilon_k)} \right]. \quad (10)$$

where η is a constant with units of square meter per watt, and is defined as

$$\eta = \frac{\epsilon_\infty^3 p^2}{\rho v_s^3}. \quad (11)$$

Note that total refractive index of the system now depends on the intensity of the acoustic wave and the material-dependent parameter η. When the intensity of the acoustic wave is zero we get back our original expression for the refractive index. Note that we have considered that the wavelength of the strain field is very large compared to photon wavelength so that the system does not have space variation in the refractive index.

Yariv and Yeh[41] have studied acousto-optic effect in homogenous medium. When acoustic wave propagate in the medium the refractive index of the medium periodically modulated both in time and space and an index grating is created. The scattering of photons with this grating gives Bragg-diffraction condition. In most calculations the time dependence of the refractive index is neglected since the frequencies of photons are much greater than the phonons frequencies.[42] In this case the system is treated as a static (frozen) periodic modulated medium.

IV. TRANSMISSION COEFFICIENT

Photons with energies lying within the photonic band gap of a photonic crystal do not propagate within it; conversely, photons with energies lying outside the photonic band gap do propagate in the photonic crystal. The photon transmission coefficient $T(\varepsilon_k)$ of the polaritonic photonic crystal is calculated using the method of Ref. 43. It is found as

$$T(\varepsilon_k) = 1 - \Phi[1 - \Lambda(\varepsilon_k)], \quad (12)$$

where $\Lambda(\varepsilon_k)$ is obtained from the photonic dispersion relation and is written as

$$\Lambda(\varepsilon_k) = \Pi_+(\varepsilon_k) + \Pi_-(\varepsilon_k), \quad (13)$$

where

$$\Pi_\pm = \left(\frac{[n_T(\varepsilon_k, I_a) \pm n_s]^2}{4n_s n_T(\varepsilon_k, I_a)} \right) \times \cos\left(\frac{2\varepsilon_k[an_T(\varepsilon_k, I_a) \pm n_s(L-2a)]}{\hbar c} \right). \quad (14)$$

Here Φ is the Heaviside step function and has the following property:

$$\Phi(x) = 1 \quad \text{for } x > 1,$$

$$\Phi(x) = 0 \quad \text{for } x < 1. \tag{15}$$

V. SPONTANEOUS EMISSION

We consider that the polaritonic photonic crystal is doped with a two-level quantum dot. Energy levels of the quantum dot are denoted as $|a\rangle$ and $|b\rangle$ where the former is the ground state and latter is the excited state. Let us consider that initially the quantum dot is in the excited state. Therefore, it is interacting with the polaritonic photonic crystal which is acting as reservoir. In the rotating wave approximation the Hamiltonian of the system is written in the interaction representation as

$$H = \left(\sigma_z + \frac{1}{2}\right)\varepsilon_{ba} + \sum_k \varepsilon_k a_k^+ a_k - \sum_{k_z}\left(\frac{\mu_{ba}}{\hbar}\sqrt{\frac{\varepsilon_k}{2\varepsilon_0 V}}\right)a_k \sigma^+ e^{i(\varepsilon_{ba}-\varepsilon_k)t/\hbar} + \text{H.c.}, \tag{16}$$

where $\sigma_z = |b\rangle\langle b| - |a\rangle\langle a|$, $\sigma^+ = |b\rangle\langle a|$, and $\sigma^- = |a\rangle\langle b|$. The operators a_k and a_k^+ are called the photon annihilation and creation operators of the reservoir, respectively. Here ε_k is photon energy in the photonic crystal and can be obtained by solving the band structure, Eq. (2), and ε_{ba}, the transition energy between states $|a\rangle$ and $|b\rangle$. The first and second terms in Eq. (16) correspond to the Hamiltonian of a quantum dot and photons in the photonic crystal, respectively. The third term describes the coupling between a quantum dot and photonic crystal. Here V is the volume of the crystal and μ_{ba} is the dipole moment of the quantum dot.

The self-energy Ξ_{ba} for the spontaneous emission can be calculated from Eq. (16) by using the Schrödinger equation method developed in Ref. 44, and is obtained as

$$\Xi_{ba} = \lim_{s\to 0^+}\int d\varepsilon_k D(\varepsilon_k)\left[\frac{\hbar(\varepsilon_k \mu_{ba})^2}{2\epsilon_0 \varepsilon_k V}\right]\frac{1}{(\varepsilon_k - \varepsilon_{ba}) - is}, \tag{17}$$

where $D(\varepsilon_k)$ is the density of states. The DOS is calculated from Eqs. (1) and (2) and found as

$$D(\varepsilon_k, I_a) = \left(\frac{Vk^2}{3\pi^2 c}\right)\frac{\xi(\varepsilon_k)}{\sqrt{1 - F^2(\varepsilon_k)}}, \tag{18}$$

where

$$\xi(\varepsilon_k, I_a) = A(\cos\theta_+ - \cos\theta_-) + B([n_T(\varepsilon_k, I_a) + n_s]^2 \sin\theta_+ - [n_T(\varepsilon_k, I_a) - n_s]^2 \sin\theta_-), \tag{19}$$

$$A = \frac{c n_T'(\varepsilon_k, I_a)[n_T^2(\varepsilon_k, I_a) - n_s^2]}{L n_s n_T^2(\varepsilon_k, I_a)},$$

$$B = \left(\frac{2a}{\hbar L}\right)\frac{[n_T(\varepsilon_k, I_a) + \varepsilon_k n_T'(\varepsilon_k, I_a)]}{4 n_T(\varepsilon_k, I_a) n_s},$$

$$\theta_\pm = \left(\frac{2\varepsilon_k}{\hbar c}\right)[n_T(\varepsilon_k, I_a)a \pm n_s(L - 2a)], \tag{20}$$

and n_T' is the derivative of n_T with respect to ε_k. Note that the DOS has a singularity where the function $F(\varepsilon_k)$ becomes unity. Generally this function becomes unity at the band edges. The DOS also depends on the intensity of the acoustic wave.

The self-energy is a complex quantity and its imaginary part [i.e., $\Gamma_{ba} = \text{Im}(\Xi_{ba})$] gives the spontaneous emission decay rate or linewidth. After some mathematical calculations we get the following expression for the linewidth:

$$\Gamma_{ba} = \gamma_0\left[\frac{\xi(\varepsilon_k, I_a)}{\sqrt{1 - F^2(\varepsilon_k, I_a)}}\right], \tag{21}$$

where

$$\gamma_0 = \frac{\mu^2 \varepsilon_{ba}^3}{3\pi\epsilon_0 \hbar^4 c^3}. \tag{22}$$

Here γ_0 is the linewidth for an energy level of an atom when it is located in a vacuum. Note that the decay rate depends on the intensity of the acoustic wave. We have shown that the DOS has very a large value near the band edges. Therefore, the spontaneous decay rate has a very large value when the resonance energy ε_{ba} lies near photonic and edges. It should be noted that asymptotic increase of the DOS at the band edges is peculiar to one-dimensional crystals and not to three-dimensional crystals. However, we want to point out that the DOS increases exponentially near the band edges in 2D and 3D photonic crystals.[45–49] In our calculations we did not use the value of DOS at the band edges.

VI. NUMERICAL CALCULATIONS

In this section numerical calculations are performed on the transmission coefficient, dispersion relation, and the spontaneous emission decay rate. We have done these calculations for four polaritonic photonic crystals fabricated from GaP, MgO, $LiNbO_3$, and $LiTaO_3$ with air. These materials are chosen since they are widely used in fabrication and characterization of polaritonic devices. The parameters used in our numerical calculations for each of the polaritonic materials are given in Table I. These parameters are taken from Refs. 3, 12, 50, and 51.

We have calculated the effective dielectric constant of the polaritonic materials as a function of incident photon energy. The results for the real part of the dielectric are shown in Fig. 1, where the solid and dashed curves correspond to GaP and MgO, respectively, and the dotted and dotted-dashed curves represent $LiNbO_3$ and $LiTaO_3$, respectively. Here we have used an experimental value of $\gamma = 0.014\varepsilon_T$ for all materials.[16]

Note that in Fig. 1, we find that all materials have a singularity in their dielectric constant near the optical photon energy when decay constant is taken as zero. However, when we consider the effect of the decay constant (i.e., $\gamma = 0.6$ meV) the singularity disappears. One can also see that the energy difference between ε_L and ε_T, which represents the inherent energy band gap in polaritonic materials, is

TABLE I. Polaritonic material constants.

Polaritonic material	ϵ_∞	ε_T (meV)	ε_L (meV)	ρ (10^3 kg/m^3)	v_s (10^3 m/s)	p
GaP	8.5	45	51	4.13	6.35	0.18
MgO	2.75	38	72	3.58	5.35	0.18[a]
$LiNbO_3$	20.6	31	65	4.7	6.57	0.29
$LiTaO_3$	13.4	18	31	7.45	6.19	0.15

[a]Note, we were unable to find reliable numbers for the photoelastic constant of MgO so the number for GaP has been used instead.

greatest for GaP and $LiNbO_3$, then $LiTaO_3$, and MgO in succession.

The results from our numerical simulations of the photonic dispersion relations for the four polaritonic photonic crystals are given in Figs. 2(a) and 2(b), where we have used the parameters $L=200$ nm and $2L/a=0.3$ for each crystal. The solid and dotted lines in Fig. 2(a) correspond to GaP and MgO, respectively. Similarly, the dashed and dotted-dashed lines in Fig. 2(b) correspond to $LiNbO_3$ and $LiTaO_3$, respectively.

The photonic band-gap width of a crystal is defined as $\Delta\varepsilon=\varepsilon_c-\varepsilon_v$, where ε_c and ε_v are the upper and lower band edges of the gap, respectively. We have calculated the photonic band-gap widths for the four polaritonic photonic crystals, which were found to be $\Delta\varepsilon_{GaP}=0.35$ eV, $\Delta\varepsilon_{MgO}=0.13$ eV, $\Delta\varepsilon_{LiNbO_3}=0.46$ eV, and $\Delta\varepsilon_{LiTaO_3}=0.42$ eV. It is interesting to note that the band gap of the $LiNbO_3$ photonic crystal has largest value whereas the band gap for MgO crystal has smallest value. The order of the band-gap widths seems to be the same as the contributions due to the high-frequency dielectric constant, ϵ_∞. Therefore, our calculations predict that the high-frequency dielectric constant has the greatest effect on the width of the photonic band gaps in polaritonic photonic crystals. MgO, though, has its band edges at the greatest energy, GaP follows with the next highest then $LiTaO_3$ and $LiNbO_3$, respectively. This varies inversely with the factor $\epsilon_\infty\varepsilon_L^2/\varepsilon_T^2$, where ε_L and ε_T are the longitudinal- and transverse-optical phonon energies.

Huang *et al.*[13] have also calculated the band structure of a photonic crystal fabricated from $LiTaO_3$ with the parameters $L=29.7$ μm and $2L/a=0.25$ and found a photonic band gap

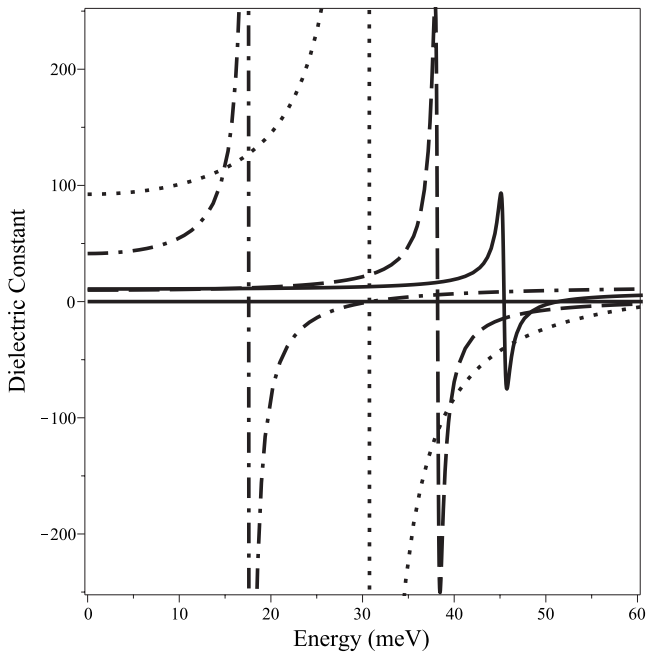

FIG. 1. The dielectric constant is plotted as function of energy. The solid curves corresponds to GaP, the dashed curve to MgO, the dotted to $LiNbO_3$, and the alternating dots and dashes to $LiTaO_3$.

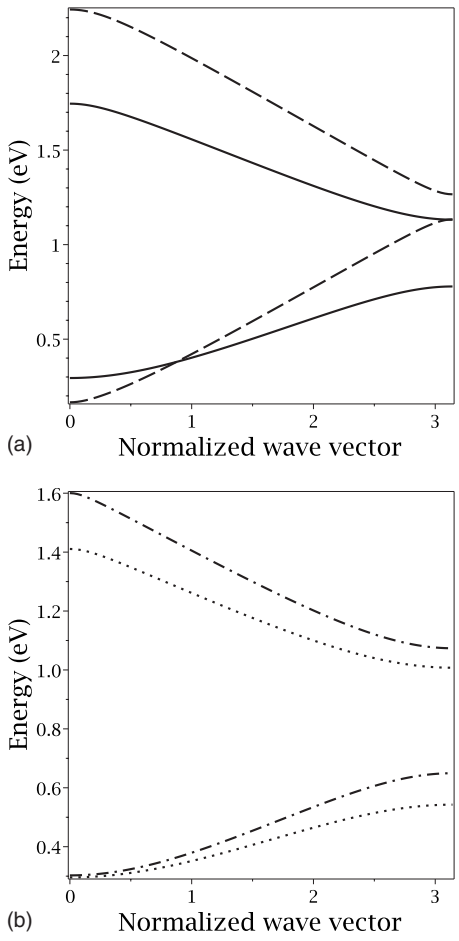

FIG. 2. The dispersion relation is plotted as function of normalized wave vector. The crystal parameters are taken as $L=200$ nm and $2L/a=0.3$. (a) The solid curves correspond to GaP and the dashed curve to MgO. (b) The dotted line corresponds to $LiNbO_3$ and the alternating dots and dashes to $LiTaO_3$.

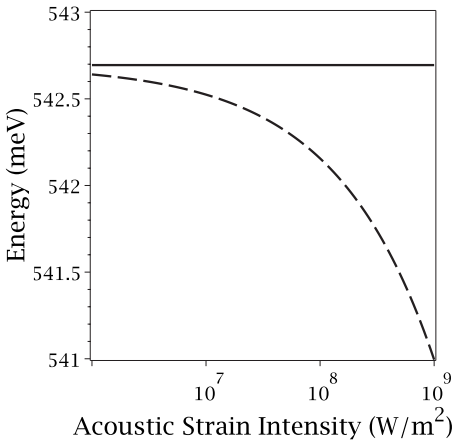

FIG. 3. The lower band-edge energy, ε_v, of GaP is plotted as a function of acoustic strain intensity. The solid line represents ε_v for $I=0$ W/m^2 and the dashed line for varying I from $I=10^6$ W/m^2 to $I=10^9$ W/m^2.

below the polariton gap. This has been verified by our method. They also found a band gap for CsI and TlCl in the same optical region for similar crystal parameters.

Generally, photonic crystals are characterized by their gap to midgap ratio. This ratio is defined as

$$R = \frac{\Delta\varepsilon}{(\varepsilon_c + \varepsilon_v)/2}.$$

We have calculated this ratio for our four polaritonic photonic crystals and found $R_{\mathrm{GaP}}=37.0\%$, $R_{\mathrm{MgO}}=11.1\%$, $R_{\mathrm{LiNbO_3}}=60.0\%$, and $R_{\mathrm{LiTaO_3}}=49.2\%$. Note that the photonic crystal made from $LiNbO_3$ has the largest value and the crystal made from MgO has the lowest value. This again seems to be related to the relative values of ϵ_∞ whose effect on the photonic band gap width is greater than the factors that effect the band-edge location.

From Fig. 2(a) we also see that the upper band edge of MgO lies just below that of GaP. One can fabricate photonic crystal waveguides or fibers by embedding an MgO photonic crystal into a GaP photonic crystal. This is an encouraging result for the study of waveguides and fibers fabricated from photonic crystals. The present calculation will help to choose the proper materials for the fabrication of these systems. Similarly in Fig. 2(b) it is found that the upper band edge of $LiNbO_3$ lies below to that of $LiTaO_3$. Therefore, we conclude that these photonic crystals can be used to fabricate photonic waveguides and fibers.

We have investigated the effect of the energy loss constant γ on the band gap of these materials. We have varied γ through realistic values $0.001\varepsilon_T$ to $0.1\varepsilon_T$.[13] It is found this constant does not have a significant effect on the photonic band gaps of these materials. This is consistent with results found by Huang *et al.*,[13] where it was predicted that the loss factor would be minimal far above ε_T.

We have studied the acousto-optic effect on the band structure of the four polaritonic photonic crystals. The results for GaP are plotted in Fig. 3, where the solid line represents ε_v for $I=0$ W/m^2 and the dashed line for varying I from $I=10^6$ W/m^2 to $I=10^9$ W/m^2. We can see that the energy difference $[\varepsilon_v(I)-\varepsilon_v(0)]$ increases with intensity. Similar results are found for both ε_v and ε_c of all materials considered in this study.

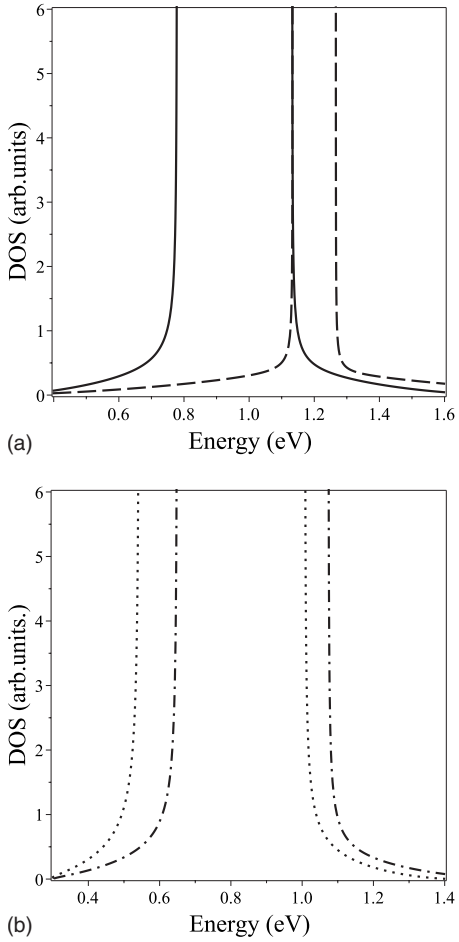

FIG. 4. The DOS is plotted as a function of photon energy of the quantum dot. The crystal parameters are taken as $L=200$ nm and $2L/a=0.3$. (a) The solid curves correspond to GaP and the dashed curves to MgO, respectively. (b) The dotted lines correspond to $LiNbO_3$ and the alternating dots and dashes to $LiTaO_3$.

We have calculated the DOS as a function of resonance energy of the quantum dot. Note that the decay rate of spontaneous emission depends on the density of states. The results from our simulations are plotted in Figs. 4(a) and 4(b) when the resonant energy ε_{ab} lies in the upper and lower bands.

In Fig. 4(a) the solid and dashed curves represent GaP and MgO polaritonic photonic crystals, respectively. Both curves have symmetric shapes in both bands. The DOS has large values near the photonic band edges for both crystals. This behavior is because the DOS has a singularity near the photonic band edges. Similarly, the DOS for $LiNbO_3$ and $LiTaO_3$ are plotted in Fig. 4(b). The dotted curve corresponds to the $LiNbO_3$ crystal whereas the alternating dashes and dots correspond to the $LiTaO_3$ crystal. For both crystals, the DOS has a singularity at the band edges.

We have considered the influence of the acousto-optic effect on spontaneous emission of the two-level quantum dot.

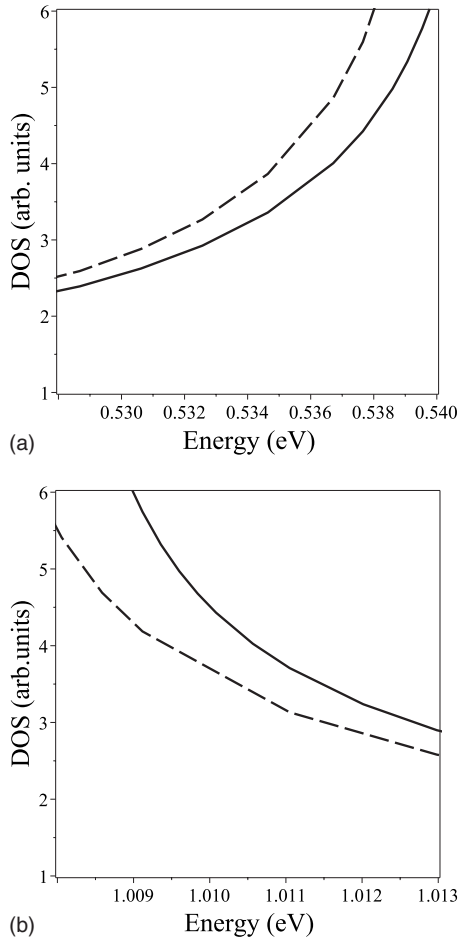

FIG. 5. The DOS is plotted as a function of photon energy of the quantum dot for varying strain intensity, I. The solid line corresponds to $LiNbO_3$ when $I=0.0$ W/m^2 and the dashed line corresponds to $I=10^9$ W/m^2 where (a) shows the lower band and (b) shows the upper band.

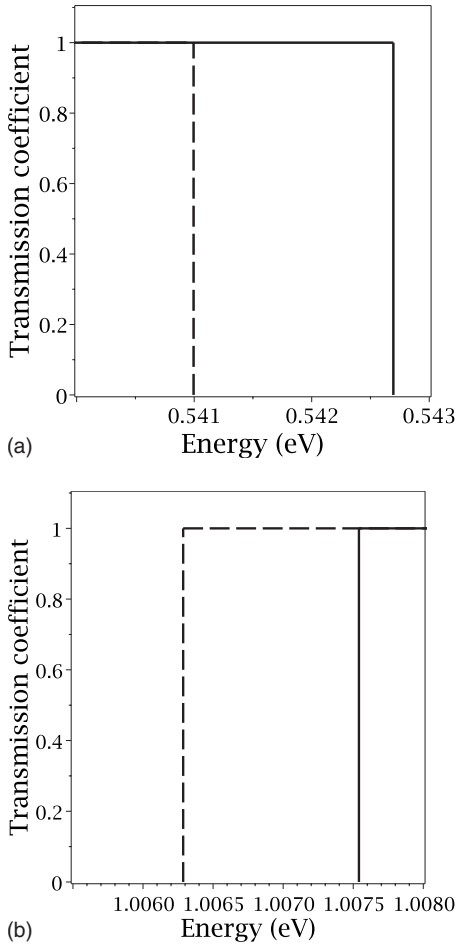

FIG. 6. The transmission coefficient is plotted as a function of energy for $LiNbO_3$. The solid curve corresponds to when strain intensity $I=0.0$ W/m^2 and the dashed curves corresponds to $I=10^9$ W/m^2. (a) shows the lower band edges and (b) shows the upper band edges.

The DOS is plotted in Figs. 5(a) and 5(b) as function strain field intensity for the $LiNbO_3$ photonic crystal. The results are plotted in separate figures because the difference between the solid and dashed curves cannot be distinguished in one figure. Similar results are also found for other crystals and are not plotted here. The solid curve is for $I=0$ W/m^2 and the dashed curve is for $I=10^9$ W/m^2. Note that in the presence of the strain field the DOS (decay rate) is modified. The decay rate is increased when the resonance energy of the quantum dot lies within the lower band. Similarly when the resonance energy lies within the upper band of the decay rate is decreased. This means that spontaneous emission of the quantum dot can be controlled by the external strain field. This is a distinct and interesting finding that is significant because spontaneous emission is the source of undesirable noise in different types of electronic and optical devices. The control of the spontaneous emission also plays a very significant role in quantum computation and quantum information processing.

The transmission coefficient of the $LiNbO_3$ polaritonic photonic crystal has been calculated as function of photon energy. Here the transmission coefficient refers to the semi-infinite crystal and not to a finite slab of it. The results are plotted in Figs. 6(a) and 6(b) and are indicated by the solid curve. These results are displayed in separate figures because the difference between the solid and dashed curves cannot be distinguished in one figure. The photonic band gap is found to be in the THz range. The lower band edge, ε_v, is located where the solid line contacts the x axis in Fig. 6(a) while the upper band edge, ε_c, is located where the solid line contacts the x axis in Fig. 6(b). Note that when the energy of photons lies below ε_v photons are able to propagate through the crystal. Similarly, when the photon energy lies above ε_c, photons propagate through the crystal. For both cases the transmission coefficient is 1. This means that the crystal is transparent for these photon energies. However, when the photon energy lies within the band gap photons are totally reflected and the transmission coefficient becomes zero. Sigalas *et al.*[15] calculated the transmission coefficient of a GaAs polaritonic photonic crystal and found the band gap in the THz region.

The acousto-optic effect has been considered in numerical calculations of the transmission coefficient of the polaritonic photonic crystal. The solid and dashed curves are plotted in

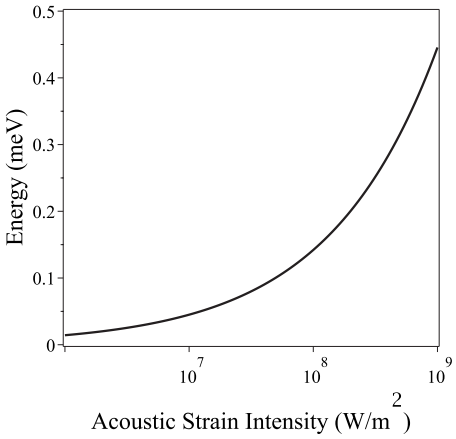

FIG. 7. The band-gap width of $LiNbO_3$ is plotted as a function of acoustic strain intensity.

the absence ($I=0$ W/m^2) and the presence ($I=10^9$ W/m^2) of the acoustic wave intensity. The presence of mechanical strain has the band-gap edges ε_v and ε_c shifted to new positions ε_v' and ε_c'. ε_v' is located where the dashed line contacts the x axis in Fig. 6(a) while ε_c' is located where the dashed line contacts the x axis in Fig. 6(b). Photons with energy just below ε_v but above ε_v' will be transmitted through the crystal in the absence of the strain field but will be totally reflected in its presence. This change is also evident for photons with energy below ε_c but above ε_c' that will be totally reflected in the absence of the strain field but will transmit when the strain field is present. This means that the system can be switched from the reflecting state to transmitting state, or vice versa depending on which band edge is used as the switch, by applying an external strain field. In other words, when the system is in reflecting state it can be considered to be in the OFF position and when the system is in a transmitting state it can be considered as ON. This is a distinct and very interesting result which can be used to fabricate switches from polaritonic photonic crystals.

We have also plotted the effect of strain-field intensity on the photonic band gap of $LiNbO_3$. The results are plotted for $[\Delta\varepsilon(I)-\Delta\varepsilon(0)]$ as a function of the strain intensity in Fig. 7. It is shown that the band gap increases as the intensity increases but the change is on the order of millielectron volt. It is found that the shift in the upper band edge due to same intensity is more than the lower band edge. Similar results are found for all materials considered in this study.

We have also examined the effect of the strain intensity on the DOS in Figs. 8(a) and 8(b) for $LiNbO_3$. Figure 8(a) depicts the lower band of the DOS. The solid line is for photon energy $\varepsilon=0.530$ eV, the dotted line for $\varepsilon=0.535$ eV, and the dashed line for $\varepsilon=0.540$ eV. It is clear that at energies closer to the band gap, the DOS is more affected by the strain-field intensity. The upper band of the DOS is shown in Fig. 8(b), where the solid line is for resonance energy $\varepsilon=1.030$ eV, the dotted line for $\varepsilon=1.035$ eV, and the dashed line for $\varepsilon=1.040$ eV. In the upper band, for energies closer to the band gap, the effect on the DOS is similar to the lower band.

Finally, we would like to make a comment on the band-structure model used in the present paper. This model was

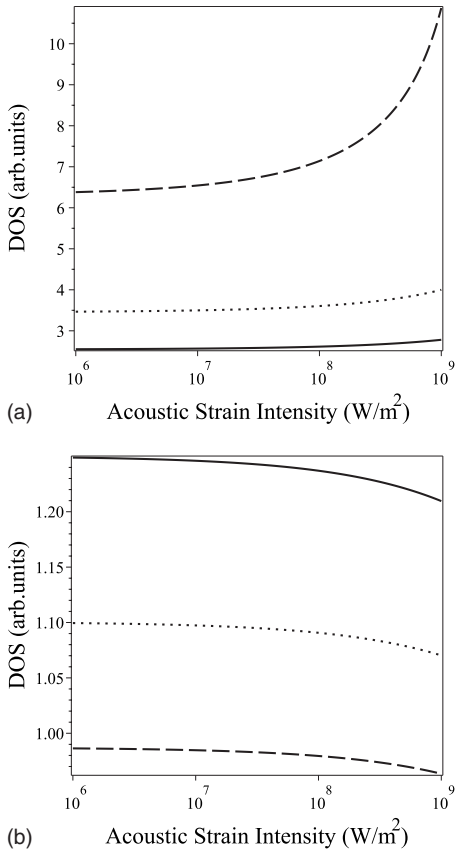

FIG. 8. The DOS is plotted as a function of acoustic strain intensity for specific values of the photon energy for $LiNbO_3$. (a) depicts the lower band of the DOS. The solid line is for photon energy $\varepsilon=0.530$ eV, the dotted line for $\varepsilon=0.535$ eV, and the dashed line for $\varepsilon=0.540$ eV. (b) shows the upper band of the DOS. The solid line is for photon energy $\varepsilon=1.030$ eV, the dotted line for $\varepsilon=1.035$ eV, and the dashed line for $\varepsilon=1.040$ eV.

proposed by John and Wang[29] and is widely used to understand the optical properties of photonic crystals because of its simplicity.[9,30–39] Typically, the band structures of 2D and 3D photonic crystals are determined with rigorous numerical approaches such as the plane-wave expansion and the transfer-matrix methods. These methods produce photonic band gaps and large values for the DOS near the band edges[45–49] but do not show an asymptotic behavior for the DOS at the edges. As one can realize, it is very complicated to use numerical band-structure methods to study spontaneous emission and photon transmission in these structures. One of the aims of the present paper is to get analytical expressions of the above quantities. It is important to note that using numerical approaches, one cannot obtain the analytical expressions we want. On the other hand, John's band-structure model is very useful because it gives an analytical expression for the spontaneous emission and transmission coefficient. These analytical expressions can be used for experimentalists to analyze their data easily or to initiate distinct experiments. The expressions derived here give a qualitative explanation of these phenomena. Therefore, the findings of the paper will not change even if one uses a numerical method for the band structure. Of course, to get a

quantitative explanation one has to use a numerical method for the band structure.

VII. CONCLUSIONS

We have investigated the acousto-optic effect on the photon transmission and spontaneous emission in a polaritonic photonic crystal. We considered that polaritonic photonic crystals are made from dielectric spheres which are arranged periodically in a background polaritonic material. The following polaritonic materials are used in our numerical calculations: GaP, MgO, $LiNbO_3$, and $LiTaO_3$. The dielectric spheres are made from air for simplicity. A two-level quantum dot is doped in a polaritonic crystal to study the spontaneous emission. The decay rate of the quantum dot due to spontaneous emission has been calculated using the Schrödinger equation. The band structures and photon transmission coefficients for these crystals have also been calculated. It is found that the band-gap widths and the decay rates of quantum dots depend strongly on the high-frequency dielectric constant, ϵ_∞, of the polaritonic crystals, while the photonic band and DOS midgaps vary inversely according to the factor $\epsilon_\infty \varepsilon_L^2 / \varepsilon_T^2$. The decay rate can be modified by applying an external strain field. The findings of this paper are significant because it is well known that the spontaneous emission is source of undesirable noise in different types of electronic and optical devices. The control of the spontaneous emission also plays a very significant role in quantum computation and quantum information processing. We have also predicted that these polaritonic photonic crystals can be switched from transmitting states to reflecting states by applying an external strain field. This result can be used to fabricate different types of photonic switches. When the system is in a reflecting state it can be considered OFF while when the system is in a transmitting state it can be considered as ON.

ACKNOWLEDGMENTS

The authors are thankful to the NSERC for financial support in the form of a research grant, and to Joel D. Cox and Ali Hatef for useful conversation.

[1] T. Feurer, N. S. Stoyanov, D. W. Ward, J. C. Vaughan, E. R. Statz, and K. A. Nelson, Annu. Rev. Mater. Res. **37**, 317 (2007).
[2] N. S. Stoyanov, T. Feurer, D. W. Ward, E. Statz, and K. A. Nelson, Appl. Phys. Lett. **82**, 674 (2003).
[3] C. Kittel, *Introduction to Solid State Physics* (Wiley, New York, 1986).
[4] M. Maragkou, A. J. D. Grundy, T. Ostatnický, and P. G. Lagoudakis, arXiv:1005.2516 (unpublished).
[5] C. A. A. Araújo, E. L. Albuquerque, P. W. Mauriz, and M. S. Vasconcelos, J. Opt. Soc. Am. B **26**, 1129 (2009).
[6] H. Inoue, K. Katayama, Q. Shen, T. Toyoda, and K. A. Nelson, J. Appl. Phys. **105**, 054902 (2009).
[7] D. W. Ward, E. R. Statz, and K. A. Nelson, Appl. Phys. A: Mater. Sci. Process. **86**, 49 (2007).
[8] I. E. Chupis, Low Temp. Phys. **30**, 968 (2004).
[9] V. I. Rupasov and M. R. Singh, Phys. Rev. Lett. **77**, 338 (1996).
[10] V. I. Rupasov and M. Singh, Phys. Rev. A **54**, 3614 (1996).
[11] M. R. Singh, Phys. Rev. B **80**, 195303 (2009).
[12] K. C. Huang, P. Bienstman, J. D. Joannopoulos, K. A. Nelson, and S. Fan, Phys. Rev. Lett. **90**, 196402 (2003).
[13] K. C. Huang, P. Bienstman, J. D. Joannopoulos, K. A. Nelson, and S. Fan, Phys. Rev. B **68**, 075209 (2003).
[14] K. C. Huang, E. Lidorikis, X. Jiang, J. D. Joannopoulos, K. A. Nelson, P. Bienstman, and S. Fan, Phys. Rev. B **69**, 195111 (2004).
[15] M. M. Sigalas, C. M. Soukoulis, C. T. Chan, and K. M. Ho, Phys. Rev. B **49**, 11080 (1994).
[16] W. Zhang, A. Hu, X. Lei, N. Xu, and N. Ming, Phys. Rev. B **54**, 10280 (1996).
[17] Y. Zeng, X. Chen, and W. Lu, Phys. Lett. A **351**, 319 (2006).
[18] H. Högström and C. G. Ribbing, Photonics Nanostruct. Fundam. Appl. **2**, 23 (2004).
[19] V. Kuzmiak, A. A. Maradudin, and A. R. McGurn, Phys. Rev. B **55**, 4298 (1997).
[20] A. Rung and C. G. Ribbing, Phys. Rev. Lett. **92**, 123901 (2004).
[21] A. Rung, C. G. Ribbing, and M. Qiu, Phys. Rev. B **72**, 205120 (2005).
[22] R. L. Chern, C. C. Chang, and C. C. Chang, Phys. Rev. B **73**, 235123 (2006).
[23] G. Gantzounis and N. Stefanou, Phys. Rev. B **72**, 075107 (2005).
[24] G. Gantzounis and N. Stefanou, Phys. Rev. B **75**, 193102 (2007).
[25] N. Courjal, S. Benchabane, J. Dahdah, G. Ulliac, Y. Gruson, and V. Laude, Appl. Phys. Lett. **96**, 131103 (2010).
[26] M. W. Haakestad and H. E. Engan, J. Lightwave Technol. **4**, 38 (2006).
[27] P. Dainese, P. St. J. Russell, N. Joly, J. C. Knight, G. S. Wiederhecker, H. L. Fragnito, V. Laude, and A. Khelif, Nat. Phys. **2**, 388 (2006).
[28] S. D. Lim, H. C. Park, I. K. Hwang, and B. Y. Kim, Opt. Express **16**, 6125 (2008).
[29] S. John and J. Wang, Phys. Rev. B **43**, 12772 (1991).
[30] P. Tran, J. Opt. Soc. Am. B **14**, 2589 (1997); S. John and M. Florescu, J. Opt. A, Pure Appl. Opt. **3**, S103 (2001).
[31] D. Petrosyan and G. Kurizki, Phys. Rev. A **64**, 023810 (2001).
[32] M. R. Singh, Phys. Rev. A **75**, 043809 (2007); Phys. Rev. B **75**, 155427 (2007); Phys. Lett. A **363**, 177 (2007).
[33] M. R. Singh, J. Phys. B **42**, 065503 (2009).
[34] P. Lambropoulos, G. M. Nikolopoulos, T. R. Nielsen, and S. Bay, Rep. Prog. Phys. **63**, 455 (2000), and references therein; K. B. Chung and S. H. Kim, Opt. Commun. **209**, 229 (2002); M. Scalora, J. P. Dowling, C. M. Bowden, and M. J. Bloemer, Phys. Rev. Lett. **73**, 1368 (1994).
[35] M. R. Singh, in *Recent Research Activities in Chemical Physics: From Atomic Scale to Macroscale*, edited by E. Paspalakis and A. F. Terzis (Transworld Research Network, Trivandrum, 2007), Chap. 5, pp. 101–165.

[36] D. G. Angelakis, E. Paspalakis, and P. L. Knight, Phys. Rev. A **64**, 013801 (2001).
[37] E. Paspalakis, N. J. Kylstra, and P. L. Knight, Phys. Rev. A **60**, R33 (1999).
[38] I. Haque and M. R. Singh, J. Phys.: Condens. Matter **19**, 156229 (2007).
[39] V. Shklover, L. Braginsky, G. Witz, M. Mishrikey, and C. Hafner, J. Comput. Theor. Nanosci. **5**, 862 (2008), and references therein.
[40] S. John, Phys. Rev. Lett. **58**, 2486 (1987); E. Yablonovitch, *ibid.* **58**, 2059 (1987).
[41] A. Yariv and P. Yeh, *Photonics* (Oxford University Press, New York, 2007).
[42] B. E. A. Saleh and M. C. Teich, *Fundamentals of Photonics* (Wiley, Toronto, 1991).
[43] M. Singh and R. Lispon, J. Phys. B **41**, 015401 (2008).
[44] M. R. Singh and W. Lau, Phys. Lett. A **231**, 115 (1997).
[45] M. Che and Z. Y. Li, Phys. Rev. B **77**, 125138 (2008).
[46] K. Busch and S. John, Phys. Rev. E **58**, 3896 (1998).
[47] M. A. Ustyantsev, L. F. Marsal, J. Ferre-Borrull, and J. Pallares, Proceedings of 2005 Seventh International Conference on Transparent Optical Networks (ICTON 2005), 2005 (unpublished), p. 315.
[48] Z. Y. Li, X. Zhang, and Z. Q. Zhang, Phys. Rev. B **61**, 15738 (2000).
[49] I. El-Kady, W. W. Chow, and J. G. Fleming, Phys. Rev. B **72**, 195110 (2005).
[50] N. J. Berg and J. N. Lee, *Acousto-optic Signal Processing* (Dekker, New York, 1996).
[51] A. S. Barker, Jr. and R. Loudon, Phys. Rev. **158**, 433 (1967).